Effect of Axial Restrained Force on Behavior and Average Crack Spacing of Reinforced Concrete Flexural Member

Seong-Tae Yi [1)], Eun-Ik Yang[2)], and Young-Ki Kim[1)]

1) Department of Civil & Architectural Engineering, Korea Power Engineering Company Inc. (KOPEC), Gyeonggi-do, Korea
2) Department of Civil Engineering, Kangnung National University, Kangwon-do, Korea

ABSTRACT

This study was performed to verify the effect of axial force and its restraint on the mechanical behavior and the average crack spacing of the reinforced concrete (RC) flexural members. Experiments have been performed on axially restrained and unrestrained RC beams for comparison of strength and rigidity of the flexural member. Furthermore, the average crack spacing has also been investigated under the axially restrained condition.

The test results showed that the flexural strength and rigidity of the axially restrained beam were higher than those of the unrestrained beam. For flexural member whose axial deformation is restrained, deformation is decreased, plastic behavior is delayed, and possibility of flexural compressive failure is increased due to the effects of axial compressive force. The major factors affecting the average crack spacing were bar stress, axial force, circumference of reinforcing bar and effective tension area of concrete. However, the effect of the concrete compressive strength was minimal. A prediction equation comprising the discussed variables is proposed for determining the average crack spacing of the axially restrained RC flexural member.

INTRODUCTION

Generally, experiments for the study of RC flexural members are performed for independent specimens without considering the effect of restraints by connected structural members. However, actual concrete members in all structures including nuclear power plant structures are under restrained conditions imposed by adjacent members or basement. These restraints make the behavior of the member vary from those of isolated members without restraining as generally studied in laboratory. To understand the effect of axial restraint on structural members, many researches were performed in the past. However, accurate experimental data is not sufficient to evaluate the restraint effects properly.

Based on the results of experiments and analyses performed until now, it is concluded that the actual behavior of any concrete members of the structural system is different from that of an individual member alone, such as test specimen, whose members separated in structures due to the change of restraining condition. From other studies (for example, Desayi and Kulkarni [1], Wight [2], Chengsheng and Wimal [3], Megget and Fenwick [4]), it is acknowledged that behaviors of RC flexural members are governed by intensity of axial restraints. The axial restraint for concrete flexural members begins with the development of hydration heat of cement at an early age and continues to the failure of members due to loading. Additionally, when the lateral load is applied to the actual concrete member, effects of free deformations and axial deformations are considered independently. Thus, a comprehensive evaluation considering those restraint conditions is required to figure out the behaviors of flexural members. However, to date, organized studies for evaluations are not performed.

To investigate systematically the behavior of flexural members restrained axially, overall evaluations considering the process restraint conditions are to be performed. In this study, the lateral load and axial load tests were conducted on the concrete beams to clarify the mechanical behavior and average crack spacing of concrete flexural members under the restrained condition.

EFFECT OF AXIAL RESTRAINT ON THE BEHAVIOR OF RC MEMBERS

Test specimen

Concrete for the beam and cylinder specimen was produced using Type I Portland cement, river sand, and crushed coarse aggregate of 15 mm maximum size. Mix proportions for concrete used in this study is shown in Table 1. The compressive strength of concrete f_c' at 28 day was 71 MPa. This value is an average of three ϕ10×20 cm cylinders in the series.

Specimens used in this study for flexural failure tests consist of two pairs of concrete beams sized 18 cm wide×25 cm high×2.4 m long. One of them is a RC beam restrained axially during testing period (FR), the other is a RC beam unrestrained (FF). To simulate the effect of cement hydration heat on specimens, all specimens were covered with glass wool sheet until demoulding. After demoulding at 3 days, all specimens were stored under a normal room condition. Beam sections

and reinforcement details are shown in Fig. 1.

Table 1. Mix proportions

w/c, %	s/a, %	W, kg/m^3	C, kg/m^3	S, kg/m^3	G, kg/m^3	Ad*, %	Air, %
27	47.7	165	611	756	857	1.1	2.6

*Admixture percentage is calculated based on cement weight.

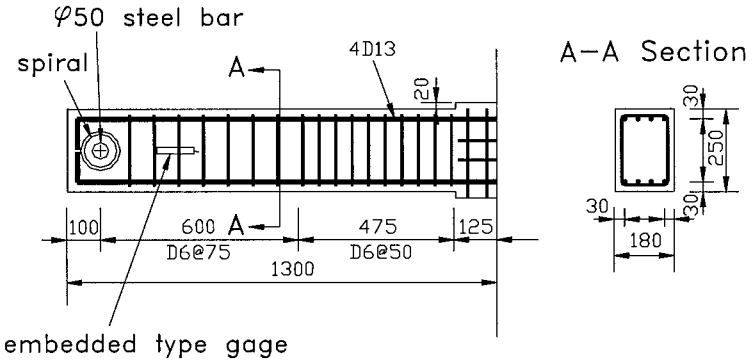

Fig. 1 Sectional area of specimens and reinforcement details

Method to impose axial deformation restraint

An automatic deformation restraining system was utilized to restrain continuously the axial deformation of specimens during loading. The outline of this set-up is shown in Fig. 2.

An hydraulic jack was used to pressurize the specimen for controlling and maintaining the strain of the displacement transducer located on both ends of the specimen within the range of a set value (axial deformation value: ±0.02 mm, conversion strain: ±8.3 μ). However, when axial restraining force due to axial deformation restraint reached 353 kN of horizontal resisting capacity, the control method was changed from the perfect axial deformation restraint to the constant axial force restraint.

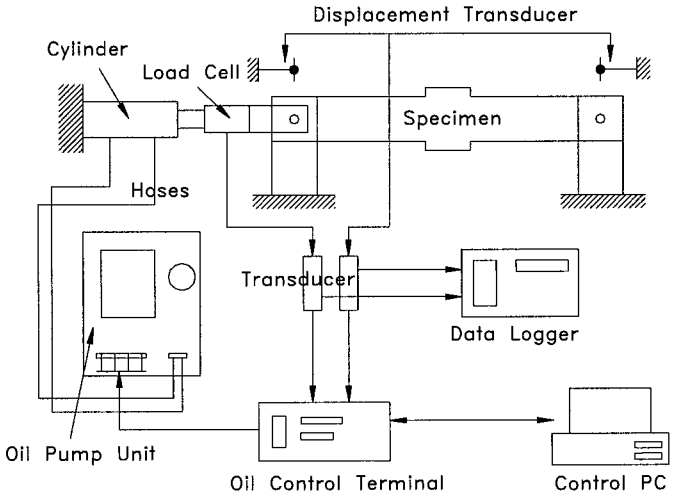

Fig. 2 Outline of organization

Loading Method

In the flexural failure test, a lateral load was applied repeatedly and the loading direction is reversed when the central

displacement at the center of member reached $0.5\Delta y^*$, Δy^*, $2\Delta y$, $3\Delta y$, $4\Delta y$, where Δy^* is displacement when the strain of main reinforcement at critical section is equal to 3,500 μ (yielding strain of longitudinal reinforcement) Δy is yielding displacement of member obtained from a load-displacement curve, and downward displacement is considered positive. As shown in Fig. 4, three points control-loading method was applied to the F series.

Relationship between lateral displacement and lateral load

Relationship between lateral displacement and lateral load of each specimen subjected to the repeated lateral load is shown in Fig. 3, where the lateral displacements of specimens mean the vertical displacements at the loading points.

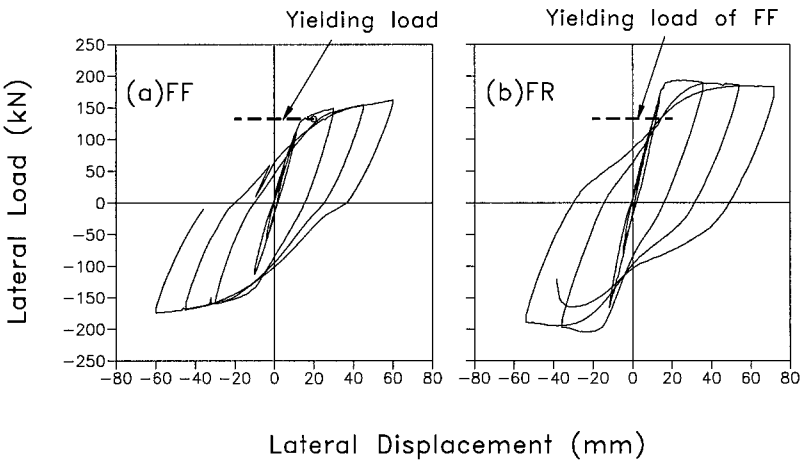

Fig. 3 Lateral load-displacement curve

Figure 3 shows that the maximum capacity of FR specimen under the restrained condition increases about 20% more than the unrestrained specimen's (FF). When the axial deformation is restrained perfectly the yielding point for FR specimen was not observed, however, the plastic deformation started as the restrained condition is changed to the constant loading condition. From the obtained load-displacement relationship, it was also noted that the axial restraints have influenced the elastic & plastic behavior, and maximum capacity of members.

Development of axial deformation and axial restraint force

Relationships between axial deformation and lateral load for FF, and correlation of axial restrained force and lateral load for FR are shown in Fig. 4 and Fig. 5, respectively.

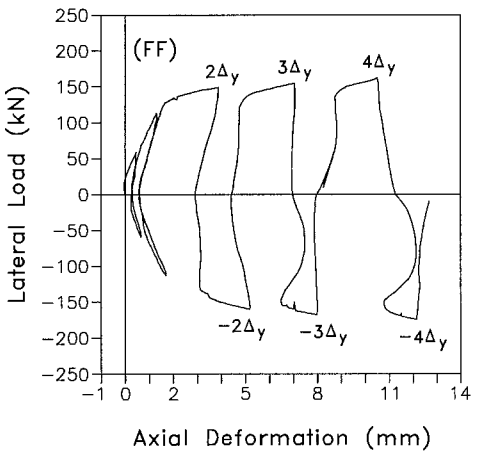

Fig. 4 Axial deformation-lateral load curve

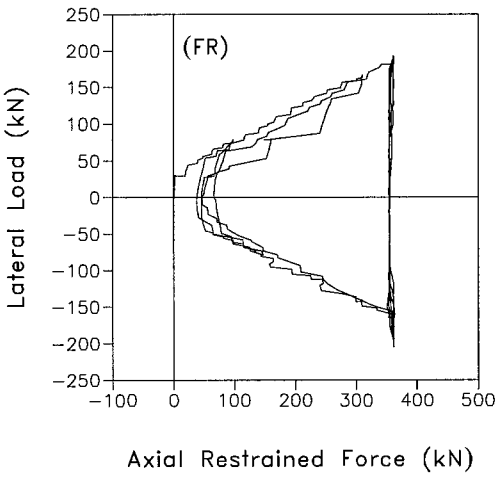

Fig. 5 Axial restrained force-lateral load curve

As shown in Fig. 4, axial deformation which began with occurrence of flexural cracks is nearly proportional to the

magnitude of lateral load within the elastic stage. After that, however, it increases rapidly with the progress of plastic deformation. When large deformation is developed, axial deformation may be inversely proportional to the lateral load, because the bond resistance mechanism toward opposite direction is formed in the slipped reinforcement of the plastic section and the deformation history of member is affected heavily by deformation of the slipped reinforcement.

According to the results of Fig. 5, when the axial deformation is restrained, axial restrained force occurs in the compressive side in proportion to the lateral load. This is because the plastic deformation of members is restrained under the perfect axial deformation restraint and axial deformation increases proportionally to the lateral load.

After loading, the crack pattern of each specimen (FF, FR) was evaluated and shown in Fig. 6. In this figure, symbol * means the initial flexural crack occurred by loading. When initial flexural cracks occurred for specimens (FF, FR) the loading values were 19.62 kN and 21.58 kN, respectively. From this it is acknowledged that each specimen shows a similar behavior because the axial restraint did not develop before the occurrence of initial flexural cracks due to absence of axial deformation.

Based on the comparison of the final crack pattern of each specimen, even though the same load history was applied, quite different crack patterns appear. For specimen FR, by axial constraints, the compressive failure phenomena are shown apparently in the vicinity of critical section. For specimen FF, however, the compressive failure occurs in the limited area. Namely, for flexural members subjected to axial load, the failure pattern of concrete members will change, and the deformation capacities will decrease. The average crack spacing and standard deviation of each specimen were (5.0 cm and 2.4 cm) and (6.4 cm and 3.1 cm), respectively. Finally, it is concluded that the crack spacing is influenced by axial force.

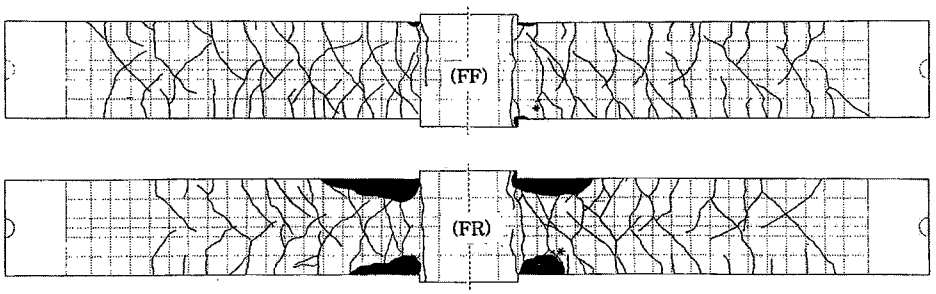

Fig. 6 Crack pattern under loading test

EFFECT OF AXIAL RESTRAINT ON THE AVERAGE CRACK SPACING OF RC MEMBERS

Test specimen

Maximum aggregate size of 13 mm in mix proportions was used. And, characteristics of test beams are shown in Table 2. All beam specimens and test cylinders were removed from the mold after 24 hours and dry-cured in a curing room for 28 days until the testing date. The f_c' value was determined based on the average of three identical ϕ10×20 cm cylinders from the same batch.

Table 2. Characteristics of test beams

No. of beam series	Type of bar	No. of bars	Sectional Area, cm^2	Perimeter of bar, cm	Effective Tension area, cm^2	f_c', MPa
I	D10	4	12×24	12	18	31
						51
II	D19	1	12×24	6	72	31
						51
III	D10	2	6×24	6	18	31
						51

Loading method

To evaluate the effect of axial force on the average crack spacing, the ultimate load was divided in 7 stages, and the

average crack spacing at the concrete tensile surface and bar location and the bar stress at each stage were measured. Bar stress was measured using the wire strain gage.

To obtain the vertical displacement with increase in loading, LVDT was installed vertically at the middle part of specimen. Four point loading method as shown in Fig. 6 was applied under the following conditions, i.e., axial force is fixed to a target value (for example, 0.07 P_u, 0.15 P_u, and 0.23 P_u), and vertical force is increased incrementally up to specimen failure. The dimensions, shape, and loading points of specimens used in the experiment are shown in Fig. 7.

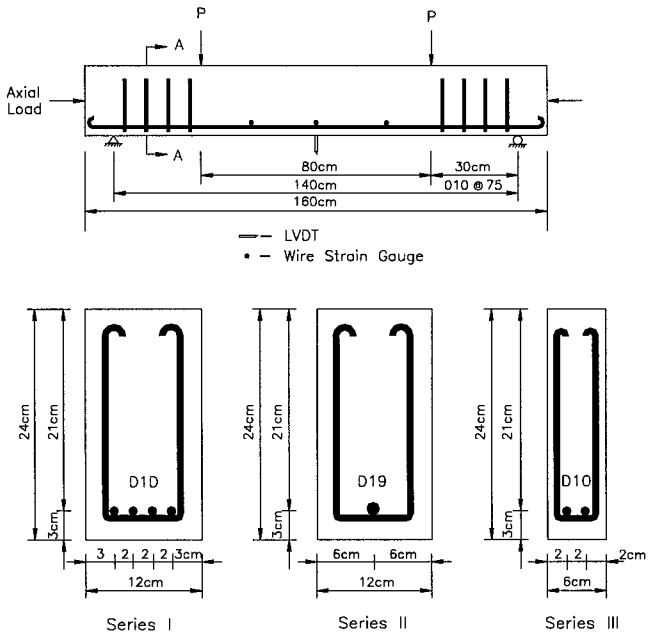

Section A-A

Fig. 7 Schematic diagram for test arrangement

To obtain a model equation which predicts the average cracking spacing, 15 shapes of specimens (30 specimens) were prepared. Since the shear failure occurred in some specimens, results of 11 shapes of specimens (17 specimens) were only available.

The parametric studies (Yang et al.[5]) for specimens selected randomly are shown in Fig. 8. From Fig. 8(a), it is observed that the intensity of axial force R_p influences in the beginning state of cracking, and the average crack spacing increases with the increase of axial load at the stabilized cracking state. Namely, the intensity of axial force affects the initial cracking occurrence and final average crack spacing. From Fig. 8(b), it is also noted that the compressive strength of concrete has very little effect on the average crack spacing at the stabilized cracking state. That is, the change of average crack spacing with the stress change of bar also proceeds independently of the compressive strength of concrete. This is because the flexural tensile strength of concrete is not proportional to the compressive strength and the concrete can not play a role as tensile materials after occurrence of cracks. According to Fig. 8(c), average crack spacing decreases when the circumference of reinforcing bar increases. That is true for all the region from the initial cracking occurrence to the stabilized cracking stage. That is because the increment of circumference of reinforcing bar means the increase of bonding area between the bar and concrete. At present some empirical equations [9,10] have adopted the effective area A_e as shown in Eq. (1). From Fig. 8(d), it can be seen that the average crack spacing increases with the increase in A_e.

$$A_e = 2(h-d)b/n \tag{1}$$

where h = overall depth of cross-section, d = effective depth, b = width of cross-section, and n = number of bar.

From the bonding characteristics of concrete and bar, the tensile force ΔT transferred from bar to concrete can be presented as Eq. (2).

$$\Delta T = f a_{cs} u_m \sum \tag{2}$$

where u_m is a function of $(f_c')^{1/2}$, f = constant presenting the distribution state of bonding stress, a_{cs} = stabilized average crack spacing (cm), u_m = maximum bonding stress, and Σ = bar circumference.

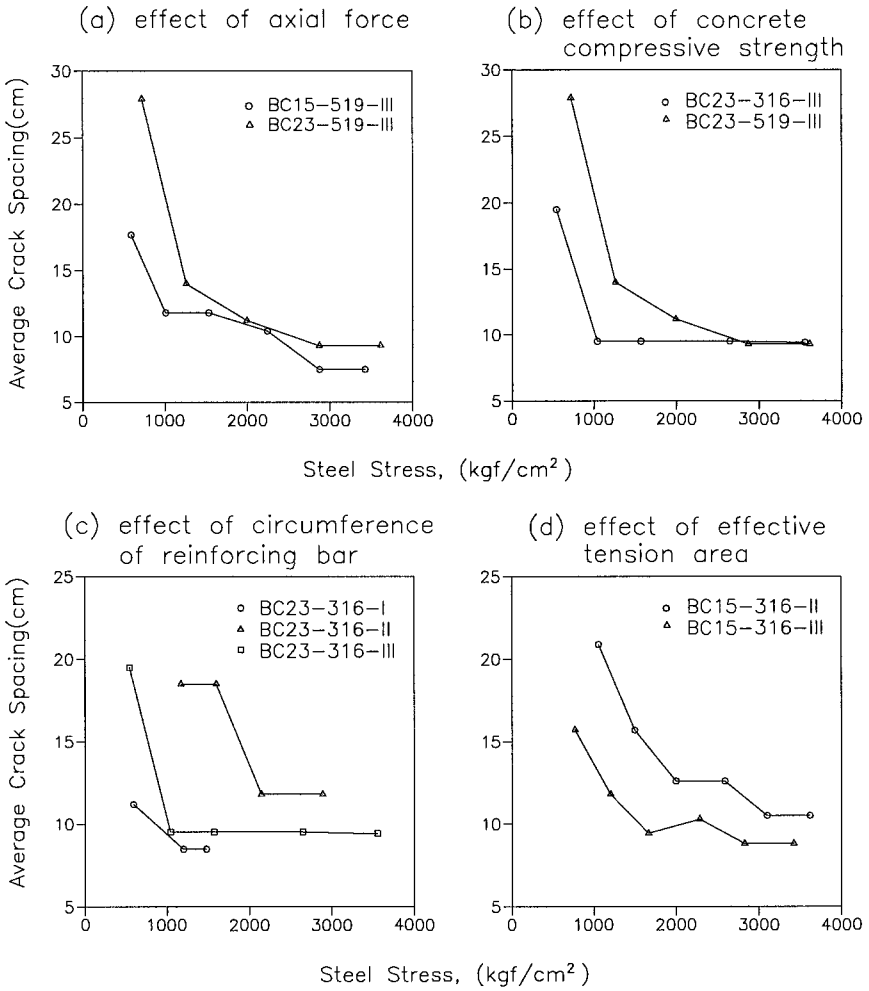

Fig. 8 Effect of major factors on crack spacing (1kgf/cm^2 = 0.0981 MPa)

Additionally, the tensile force R can be represented by multiplying A_e to the tensile strength f_t', and from the relationship of $\Delta T=R$, the following equation can be obtained.

$$a_{cs} = c_1' \frac{A_e f_t'}{\sum \sqrt{f_c'}} \tag{3}$$

where c_1' = experimental constant.

Average crack spacing is practically not affected by f_c' and $f_t'/(f_c')^{1/2}$ is a constant. Thus, Eq. (3) can be replaced by Eq. (4).

$$a = c_1 \frac{A_e}{\sum} \tag{4}$$

From Eq. (4), the average crack spacing at the stabilized state can be represented as a function of A_e/Σ, and CEB-FIP model code 1990[11] also adopt this type. However, crack spacing can also be changed apparently by axial force R_p and the effect of bar stress f_s is distinct at the initial cracking spacing.

Comparisons of measured and calculated values

To obtain a model equation, the regression analyses [12,13] were performed using the total 73 data. At this time, axial force, effective area of concrete A_e, bar stress f_s, and ratio of applied axial load to ultimate axial load of cross-section R_p were selected as major variables. According to the results of experiment, average crack spacing approaches infinite when the bar stress is very small. And, the crack spacing decreases with the increase of stress in bar, and finally converges a constant value. The spacing increases with the increase in R_p. With the foregoing considering, the following equation was obtained from the regression analyses:

$$S_{cr} = 5.5\left[\frac{A_e}{\sum}\right]^{0.3} \frac{3\times10^5 + f_s^2}{f_s^2}(1 + R_P^{0.75}) \tag{5}$$

where S_{cr} = average crack spacing (cm)
f_s = stress of bar (kgf/cm^2)

Results of regression analyses to compare Eq. (5) with experimental data are shown in Fig. 9. Comparison indicates that the proposed equation gives a good prediction. Standard deviation and correlation coefficient are 1.599 and 0.74, respectively. In this figure, thick line and thin lines present a linear equation of $y = 0.968x + 0.389$ and region of standard deviation, respectively. Even though there is more or less scatters between calculated and measured values, the linear relationship exists approximately.

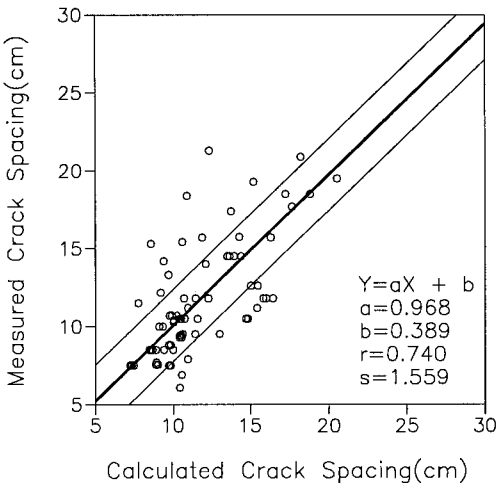

Fig. 9 Comparison of the measured and calculated values of crack spacing

In Fig. 10, comparisons of proposed equation with experimental data selected randomly are shown. In this figure, thick solid line represents the equation. It is found that the equation overestimates a little over the experimental results, but, predicts well the general trend of average crack spacing.

SUMMARY AND CONCLUSIONS

A study was performed quantitatively to evaluate effects of the axial force, occurring due to axial restraints, on the mechanical behavior and average crack spacing of RC flexural members. From the test results and analyses, the following conclusions are drawn.

1) Rigidities of flexural members subjected to axial deformation restraints are bigger than those of unrestrained members because axial compressive force increases in proportion to applied lateral force.
2) Maximum capacities of flexural members loaded on condition of axial deformation restraints are increased by about 20 % more than unrestrained members.
3) For flexural members subjected to axial compressive force, compressive failure phenomena at failure were distinct because the flexural deformation was limited.
4) Average crack spacing of flexural members subjected to axial compressive force is influenced by axial force, and the spacing is decreased, which approaches a constant value with the increase of axial force.
5) A model equation is suggested for predicting the average crack spacing of flexural members subjected to axial force.

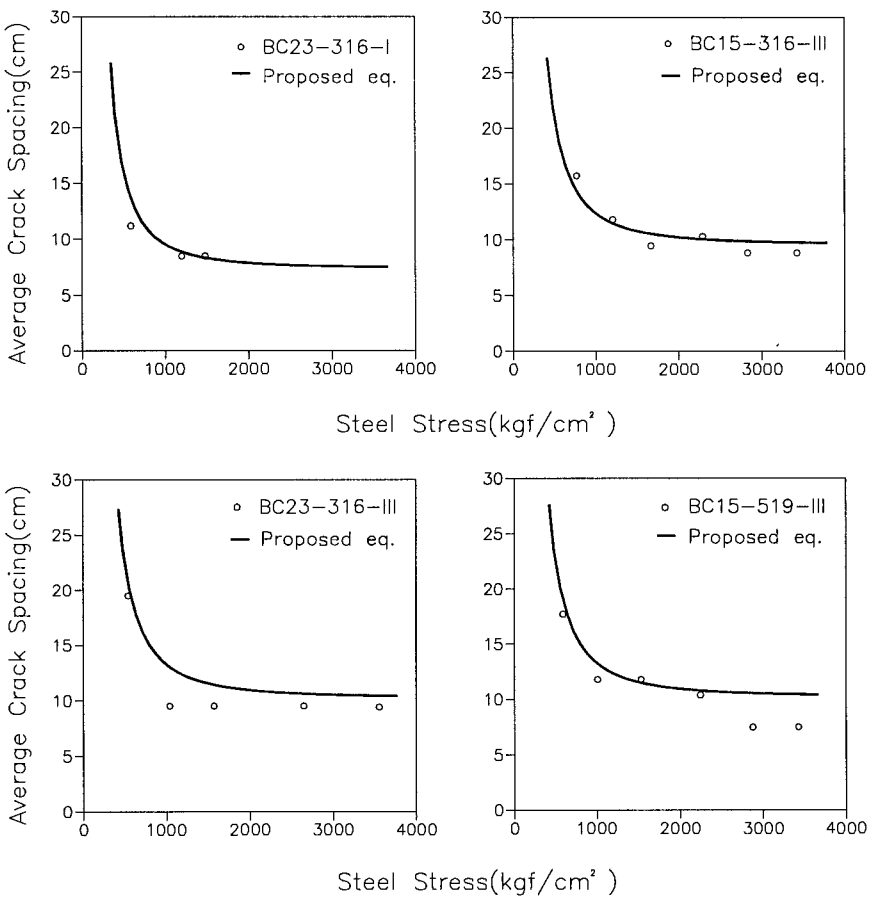

Fig. 10 Comparisons of proposed crack spacing equation with experimental data (1kgf/cm^2 = 0.0981 MPa)

REFERENCES

[1] Desayi, P. and Kulkarni, A.B., "Load - Deflection Behavior of Restrained R/C Slabs," J. of Structural Engineering, ASCE, Vol.103, No.2, Feb. 1977, pp.405-419.

[2] Wight, J.K., "Earthquake Effects on Reinforced Concrete Structures," ACI, SP84, 1985, 428p.

[3] Chengsheng, O. and Wimal, S., "RC Rectangular Slabs with Edge Restraints," J. of Structural Engineering, ASCE, Vol.113, No.11, Nov. 1987, pp.2146-2165.

[4] Megget, L.M. and Fenwick, R.C., "Seismic Behavior of a Reinforced Concrete Portal Frame Sustaining Gravity Loads," Bulletin of the New Zealand National Society for Earthquake Engineering, Vol.22, No.1, 1989, pp.39-49.

[5] Yang, E.I., Kim, J.K., Yi, S.T. and Morita, S., "The Effect of Axial Force on the Behavior and Average Crack Spacing of Reinforced Concrete Flexural Member", Journal of the Korea Concrete Institute, Vol.9, No.4, 1997, pp.207-214. (in Korean)

[6] Yang, E.I., Morita, S. and Yi, S.T., "Effect of Axial Restraint on Mechanical Behavior of High Strength Concrete Beams", ACI Structural J., Vol.97, No.5, Sep.-Oct. 2000, pp.751-756.

[7] Gergely, P. and Lutz, L.A., "Maximum Crack Width in Reinforced Concrete Flexural Members", Causes, Mechanism, and Control of Cracking in Concrete SP-20, Detroit, ACI, pp.87-117, 1968.

[8] Bazant, Z.P. and Oh, B.H., "Spacing of Cracks in Reinforced Concrete", J. of Structural Engineering, ASCE, V.109, No.9, Sept. 1983, pp.2066-2085.

[9] Hognestad, E., "High Strength Bars as Concrete Reinforcement, Part 2, Control of Flexural cracking", J. of PCA, V.4, No.1, Jan. 1962, pp.46-63.

[10] Albandar, F. A-A. and Mills, G. M., "The Prediction of Crack Widths in Reinforced Concrete Beams", Magazine of Concrete Research, V.26, No.88, Sept. 1974, pp.153-160.

[11] CEB, CEB-FIP Model Code 1990, Thomas Telford, 1991.

[12] IMSL, Library, Edition 8, IMSL, Inc.

[13] Benjamin, J.R. and Cornell, C.A., "Probability, Statistics, and Decision for Civil Engineers," McGraw-Hill Publishing Company, New York, 1970, Section 4.3.